IOP PUBLISHING PLASMA PHYSICS AND CONTROLLED FUSION

Plasma Phys. Control. Fusion **49** (2007) 619–629 doi:10.1088/0741-3335/49/5/004

Sensitivity of electron temperature measurements with the tunnel probe to a fast electron component

T Van Rompuy[1,4], J P Gunn[2], R Dejarnac[3], J Stöckel[3] and G Van Oost[1]

[1] Department of Applied Physics, Ghent University, Rozier 44, Ghent B-9000, Belgium
[2] Association CEA-EURATOM sur la fusion contrôlée, Saint Paul Lez Durance F-13108, France
[3] Institute of Plasma Physics, Association EURATOM-IPP.CR, Za Slovankou 3, 18200 Prague 8, Czech Republic

E-mail: thibaut.vanrompuy@ugent.be

Received 3 October 2006, in final form 28 February 2007
Published 26 March 2007
Online at stacks.iop.org/PPCF/49/619

Abstract

The tunnel probe is a new kind of Langmuir probe for fast dc measurements of ion flux and electron temperature in the tokamak scrape-off layer. The probe is calibrated using two-dimensional kinetic analysis of the ion current distribution on the concave conductors. Though qualitative agreement with classical Langmuir probe measurements was found, the electron temperature given by the tunnel probe is several times lower. One possible explanation might be an overestimation of the electron temperature by the Langmuir probe, due to a non-Maxwellian electron velocity distribution which can be modelled in a first approach as a two-temperature distribution. Hence the possible influence on the tunnel probe of a small population of nonthermal electrons is investigated by means of the two-dimensional kinetic code XOOPIC. It is found that this influence can be seen as the result of two combined physical effects: nonthermal electrons will reach the back plate (BP) and the ion current distribution over tunnel and the BP will change. The resulting dependence on probe bias and parallel ion current density of the TP sensitivity to nonthermal electrons is not reflected in CASTOR measurement results. Thus nonthermal electrons on their own cannot fully explain the discrepancy between Langmuir and tunnel probe measurements.

1. Introduction

To study turbulence in a tokamak edge plasma by means of probes, it is important to be able to measure electron temperature T_e and parallel ion current density $J_\parallel$ with high frequency [1]. A new kind of plasma probe, the tunnel probe, provides simultaneous measurements of T_e and $J_\parallel$.

[4] Author to whom any correspondence should be addressed.

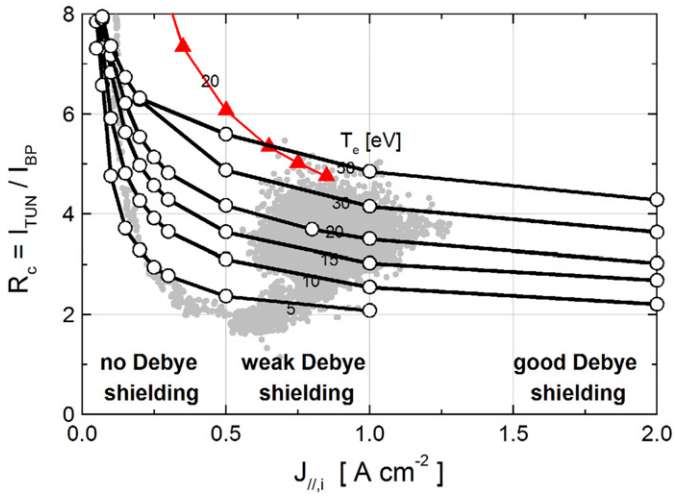

Figure 1. The lines with open circles are simulated tunnel-to-back plate ion current ratios for various values of $J_{\|,i}$ and Te assuming hydrogen, $B = 1$ T, tunnel diameter and depth both 5 mm, and applied voltage -100 V. The grey points are measured (CASTOR shot 13172). Simulation results for $T_e = 20$ eV, $V = -200$ V are shown for comparison (full triangles).

(This figure is in colour only in the electronic version)

It operates in dc, thus avoiding electronic equipment frequency limitations in fast-sweep single probe techniques.

The tunnel probe [2–4] consists of two negatively biased conducting surfaces which are electrically isolated from each other: a hollow tunnel with a diameter of a few millimetres and a back plate (BP) closing one end of the tunnel. This geometry is illustrated in figure 1 of [4]. The axis of the tunnel is parallel to the magnetic field $\boldsymbol{B}$. Plasma flows into the open side of the tunnel and the flux is distributed between the tunnel and the BP. The ratio R_c of the two resulting currents to tunnel (I_{TUN}) and BP (I_{BP}) is strongly determined by the strength and distribution of the electric field inside the tunnel, and should be, according to magnetic sheath (MS) theory [5–6], a strong function of T_e. For a fixed value of $J_\|$, an increase in T_e will cause an increase in the radial electric field in the tunnel and more ions will be demagnetized and attracted to the tunnel surface before they can reach the BP, thus raising R_c. As the penetration of the probe potential into the tunnel plasma depends on the plasma density, the fraction of ions that will be scraped off to the tunnel will change for a different $J_\|$. To calibrate the probe, we determine the theoretical relation between R_c on the one hand and T_e, $J_\|$ and the probe biasing potential V_{bias} (as compared with the floating potential V_f) on the other hand, using the self-consistent, two-dimensional kinetic code XOOPIC [7]. Calibration results are shown in figure 1 [3].

In order to investigate the validity of the calibration simulation results, measurements with a prototype TP were made in the CASTOR tokamak [8]. For those experiments, the voltage on all conductors of the tunnel probe was swept and the obtained current–voltage (I–V) characteristics were used to give two independent measurements of T_e. Firstly, the sum of the collected currents resulted in an I–V characteristic which is equivalent to that of an ideal disc Langmuir probe. The T_e was obtained in the usual way by making a non-linear 3-parameter fit to the function

$$I = I_{SAT}\left(1 - \exp\left(\frac{e\,(V - V_f)}{kT_e}\right)\right).$$

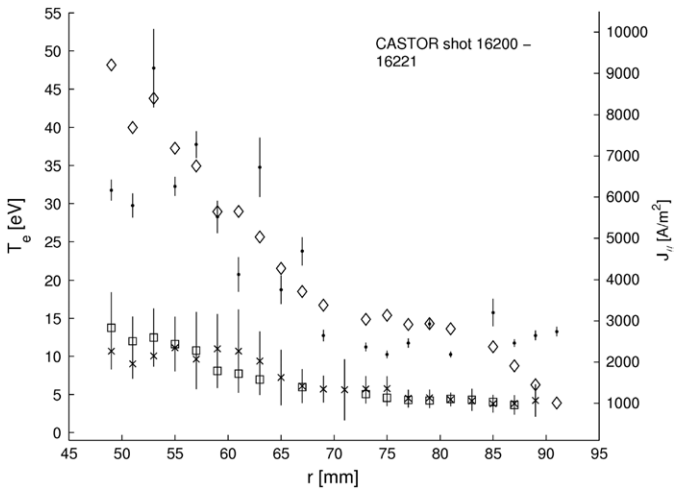

Figure 2. Radial profiles of T_e measured with a LP (dots), a TP biased at −100 V (crosses) and a TP at −200 V (squares) in the tokamak CASTOR. The $J_\parallel$-values which were measured at the same locations are shown on the right axis (diamonds).

Secondly, the ratio of I_{TUN} and I_{BP} at very negative voltages was interpolated within the XOOPIC results of figure 1. In this way simultaneous and independent Langmuir and tunnel probe measurements of T_e were achieved. An example of radial profiles for T_e and $J_\parallel$ which were obtained using this procedure during Ohmic discharges, is given in figure 2. Although the TP and LP T_e-measurements show good agreement qualitatively, the values derived from the TP technique were generally found to be a few times lower than the LP values.

Several mechanisms could be thought of as at least partially causing this difference in absolute TP and LP T_e-measurements. Among those are effects due to rectification of plasma fluctuations, plasma resistivity in the current channel between the probe and the reference electrode (both of which would cause the LP to produce falsely high T_e-measurements) and secondary electron emission from ion bombardment of the copper BP of the TP (resulting in falsely low values of T_e measured by the TP). Another possible explanation for the difference in measured T_e-values might be an overestimation of T_e by the Langmuir probe, due to a non-Maxwellian distribution of the electrons. In a first approach this can be modelled as a two-temperature electron velocity distribution, consisting of a small, hot electron population superimposed on the bulk of the thermal electrons. This paper only investigates this last mentioned possibility, which, at first glance, is not so far-fetched, as a swept LP is sensitive to the characteristic energy of nonthermal electrons [9,10], high temperature nonthermal electrons might exist on the closed field lines in the plasma and scrape-off layer (SOL) electrons might not be Maxwellian in low or intermediate collisionality regimes (such as for the results in figure 2) [11]. The presence of non-Maxwellian electrons in CASTOR is made even more likely by the observation that for some Ohmic discharges (different from those of figure 2) simultaneous electron temperature and floating potential measurements with two swept tunnel probes, one facing the ion side and the other the electron side, gave different results, implying an anisotropic electron velocity distribution in the edge plasma of CASTOR [12].

The plausibility of this last explanation depends on the sensitivity of the TP to this same small population of nonthermal electrons. This sensitivity would have to be notably lower than for the LP and is investigated in this paper by means of XOOPIC simulations. A difference

in sensitivity is very probable, as the mechanisms by which T_e is measured are fundamentally different for TP and LP. Langmuir probes obtain T_e from analysis of the electron current to the collecting surface of the probe, assuming Boltzmann relations. The tunnel probe, on the contrary, measures T_e without collecting any electrons (if the bias is strong enough); it is the distribution of the ion current over the tunnel and BP which depends on the electric field $\boldsymbol{E}$ inside the tunnel, which in turn depends on T_e, again through the Boltzmann relation.

2. Simulation model

The XOOPIC code was run under a Linux environment on a personal computer for the CASTOR tunnel probe geometry with a tunnel diameter of 5.0 mm and a depth of 5.0 mm.

The simulation domain is the r–z plane in a cylindrical coordinate system whose axis corresponds to the axis of the tunnel (as in figure 5 of [2], but with different dimensions). The magnetic field $\boldsymbol{B}$ of 1 T is oriented parallel to this axis and towards the BP. Cell sizes and time step are chosen in accordance with standard numerical stability criteria governed by the Debye length and plasma frequency [13].

The tunnel and BP are simulated as conductors divided by a gap of 0.5 mm. The tunnel/injection plane and BP/tunnel gaps are simulated as insulators on which impinging charges are neutralized. Maxwellian fluxes of ions (i.e. protons for the simulations we describe here) with temperature T_i, thermal electrons with temperature $T_{e,\mathrm{therm}} = T_i$ and nonthermal electrons (temperature $T_{e,\mathrm{supr}}$) are injected towards the tunnel from the plane situated 1 mm to the right of the tunnel entrance. The potential of the flux injection plane is held at 0 V. In order to guarantee quasi-neutrality (within the limits of time-dependent density fluctuations that occur even when the simulation is stable) at the entrance of the tunnel, the fluxes of injected electrons and ions are adjusted so as to account for the repulsion of almost all electrons, the absorption of almost all ions and the different thermal velocities of ions and electrons. A thin source sheath forms in front of the injection surface. As the fluxes of thermal and nonthermal electrons are influenced differently by this sheath, the density fraction of nonthermal electrons reaching the probe is determined from the simulated electron densities after the source sheath.

Simulations were made with the conductors biased to −200 and −100 V relative to floating potential. Those biasing voltages were selected because of the availability of results from simulations without nonthermal electrons for those specific voltages [8]. V_f depends on the ratio of fast electron density to slow electron density and was calculated for each simulation by solving the transcendental equation (assuming no secondary electron emission): [14]

$$e^{V_f} + f_T^{1/2} f_n e^{V_f/f_T} = (f+1)^{1/2} \left(\frac{\pi m_e}{2m_i}\right)^{1/2} (1+f_n)\,,$$

where $f_T = T_{e,\mathrm{supr}}/T_e$, $f_n = n_{e,\mathrm{supr}}/n_{e,\mathrm{therm}}$ and $f = f_T(1+f_n)/(f_n+f_T)$; m_i and m_e are respectively the ion and the electron mass and $n_{e,\mathrm{supr}}$ and $n_{e,\mathrm{therm}}$ the nonthermal and thermal electron densities.

The axis, conductors, insulators and injection plane together determine the boundary conditions. For each simulation case, we run the code until the number of particles from each of the three different populations in the simulation domain becomes stable. Then the code is left to run again for roughly the same time to build up acceptable particle statistics. The charges collected by the tunnel and BP are recorded and divided by the simulation period to obtain I_{TUN} and I_{BP}. By using the TP calibration from [8] (i.e. without nonthermal electrons) the T_e which would have been measured with the TP is derived from the sum and the ratio of I_{TUN} and I_{BP}.

In conformity with plasma conditions in the edge of CASTOR, simulations were run for parallel ion fluxes of 2500 A m^{-2} and 10 000 A m^{-2} (in order to simulate in both regimes of good Debye shielding and poor Debye shielding [8], while keeping computation times reasonable), ion and thermal electron populations at 10 eV and the nonthermal electrons at 20, 50 and 100 eV, respectively. The density fraction of nonthermal electrons after the injection sheath was increased until T_e measured by the TP or the LP (whichever occurred first) equalled the T_e of the nonthermal population.

3. Simulation results and discussion

Figure 3 shows both the normalized T_e-values one would measure with the TP (downward pointing triangles) and with a LP (crosses) as a function of the nonthermal electron population density fraction ($F_{e^-,\mathrm{supr}}$) for six different combinations of plasma conditions, temperatures of the nonthermal electron population and tunnel probe biasing voltages. T_e-values were normalized to the T_e-value obtained without nonthermal electrons. To determine the T_e-values that would be measured by the LP, I–V characteristics normalized by the ion saturation current I_{SAT} have been generated using the expression derived from [14]

$$\frac{I_{tot}}{I_{SAT}} = 1 - \sqrt{\frac{2m_i}{\pi\,(1+f)\,m_e}}\,\frac{1}{1+f_n}\left(e^{\frac{eV}{kT_{e,\mathrm{therm}}}} + \sqrt{f_T}\,f_n e^{\frac{eV}{f_T kT_{e,\mathrm{therm}}}}\right).$$

To those characteristics the fit-routine used in [8] for the classical swept LP technique was applied. The thus obtained effect of the nonthermal electron population on the LP measurements is similar to the results obtained by Stangeby [9], i.e. a nonthermal electron component of just 2% by density at 10 times T_e of the thermal electron population would give a LP characteristic which could not, in practice, be distinguished from the characteristic which would result if 100% of the electrons were fast. From the calibration simulations we know that for $J_{//} = 2500$ A m^{-2} (poor Debye shielding case) the Debye sheath thickness is significant with respect to the tunnel radius, resulting in a R_c which varies much more strongly with T_e and $J_\parallel$ than for $J_\parallel = 10\,000$ A m^{-2} (good Debye shielding case). Therefore, we first discuss cases (*a*), (*b*), (*c*) and (*d*) with higher ion fluxes and good Debye shielding.

For $J_\parallel = 10\,000$ A m^{-2} and at a biasing voltage of -200 V (cases (*a*), (*b*) and (*c*)) the LP is clearly always more sensitive to small nonthermal electron populations than the TP. Hence a nonthermal electron population at 100 eV of around 0.5% density fraction (case (*a*)) or at 50 eV of 1.5% density fraction (case (*b*)) would suffice in order to obtain LP measurements which are at least 2 times higher than the TP measurements. A nonthermal electron population at 20 eV (case (*c*)) can never cause the LP measurements to be more than 40% higher than the TP measurements.

The effect of the nonthermal electron population on the TP is nevertheless quite important, which raises the need to find out through which mechanism this influence is exerted. This task is made easier by using an important advantage of simulations, namely that unlike real-world measurements, they allow us to study the separate contributions of ions and electrons to the currents collected by the tunnel and the BP. The simulation results for the TP (downward pointing triangles) shown in figure 3 have been obtained by considering the total current to the BP (both ions and electrons) as would be measured during experiments. However, we can also take only the ion current (and no electron current) to the BP into account when computing the measured T_e from the results of the TP simulations with different levels of nonthermal electron density fractions. The results are depicted in (*a*), (*b*), (*d*) and (*e*) of figure 3 as upward pointing triangles. It is clear that the effect of nonthermal electrons with a high temperature (100 eV) on the measured T_e-values is mostly a result of the flow of an electron current which has the effect

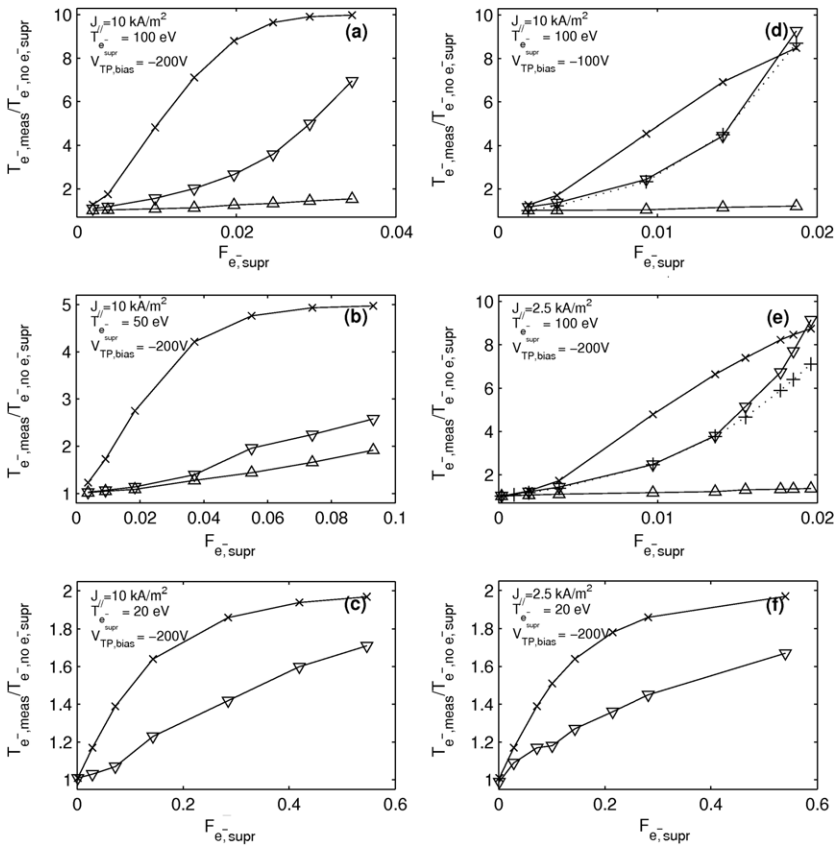

Figure 3. Normalized T_e, as would be measured by LP and TP, as a function of the e^-_{supra} density fraction for different plasma, nonthermal electrons and probe parameters. $T_{e,therm}$ is 10 eV in all cases. The LP values are marked with crosses; the TP values without and with correction for the electron current to the BP respectively with downward and upward pointing triangles. The crosses in (*d*) and (*e*) represent the relative TP T_e-values produced by considering the undisturbed ion current distribution and adding the BP nonthermal electron current which is given by applying the nonthermal electron current scaling rules to the BP nonthermal electron current in case (*a*).

of decreasing the magnitude of the BP current and increasing R_c. On the other hand, 20 eV nonthermal electrons do not have sufficient energy to reach the BP, so correcting the T_e-values obtained from the results of the TP simulations by eliminating the electron current to the BP makes no difference for cases (*c*) and (*f*) and therefore no 'corrected' TP T_e-measurement values are shown on the graphs for those cases. The effect of the nonthermal electrons on the TP T_e-measurements is thus for 20 eV nonthermal electrons entirely due to the change in distribution over the tunnel and BP of the ions.

The relative change in the ratio of the tunnel current to the BP ion current for the different cases of figure 3 is presented in figure 4. It is interesting to note that for equal $J_\parallel$, the behaviour of the dependence of R_{ion} on $F_{e^-,supr}$ is similar, but the scaling is different. Another remarkable feature is the almost identical behaviour of the cases $V_{TP,bias} = -200$ V and $V_{TP,bias} = -100$ V with $J_\parallel = 10\,000$ A m^{-2} and $T_{e,supr} = 100$ eV. The ion current distribution will change because it depends on the strength and the distribution of the electric field inside the tunnel. This electric field is mostly determined by the Boltzmann screening of electrons, which are characterized by

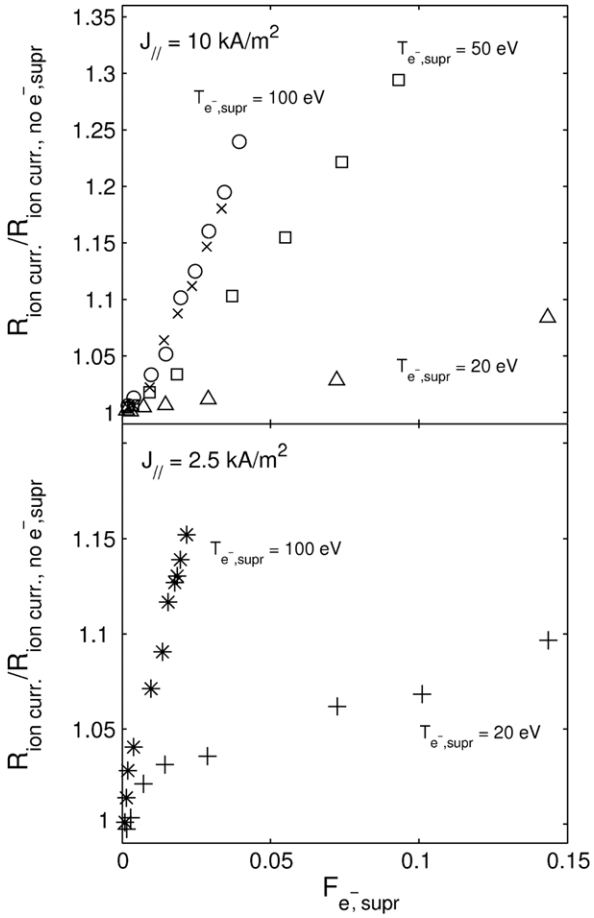

Figure 4. Relative change of the ratio of the tunnel current to the BP ion current for different cases. All the cases have $T_{\mathrm{e,therm}} = 10\,\mathrm{eV}$ in common. In the upper graph, circles and crosses represent the cases $V_{\mathrm{TP,bias}} = -200\,\mathrm{V}$ and $V_{\mathrm{TP,bias}} = -100\,\mathrm{V}$, respectively.

the 'effective' or 'screening' temperature [15, 16]. The variation of $F_{\mathrm{e}^-,\mathrm{supr}}$ will influence the effective temperature in front of the tunnel wall. The screening temperature T_{es} is determined for general electron energy distribution functions as follows:

$$T_{\mathrm{es}} = 2\left(\int_0^\infty \varepsilon^{-1/2} f\,(\varepsilon)\,\mathrm{d}\varepsilon\right)^{-1}$$

and for a bi-Maxwellian electron energy distribution function, as has been used for the simulations, this can be written as

$$T_{\mathrm{es}} = \frac{T_{\mathrm{e,supr}} T_{\mathrm{e,therm}}}{T_{\mathrm{e,therm}} F_{\mathrm{e^-supr}} + \left(1 - F_{\mathrm{e^-supr}}\right) T_{\mathrm{e,supr}}}.$$

It should be emphasized that in the case of non-Maxwellian particles, the screening temperature does not agree with the usual energetic temperature definition. As the potential distribution around the probe surfaces and the Debye length are governed by T_{es}, $F_{\mathrm{e}^-,\mathrm{supr}}$ will thus locally influence the width of Debye and magnetic sheath through its effect on T_{es}.

For nonthermal electrons with an intermediate temperature (50 eV, case (*b*) of figure 3) both mechanisms (i.e. electrons reaching the BP and a change in the ion current distribution) have a comparable contribution to the net effect.

The influence of nonthermal electrons reaching the BP is further illustrated by graph (*d*) of figure 3, where the only difference with graph (*a*) is that the simulated TP was biased at −100 V instead of −200 V. We notice that at lower biasing voltages the tunnel probe becomes clearly more sensitive to the nonthermal electrons (even more sensitive than the LP from a certain $F_{e^-,supr}$ value), because it becomes easier for electrons to reach the BP.

Between the TP and LP measurements of T_e in CASTOR there can be a relative difference of a factor of 2 up to 3, as illustrated in figure 2. From what we have learned up to this point concerning the influence of nonthermal electrons on the TP under different circumstances, we can conclude that this difference can only be explained entirely (i.e. without having to combine it with other possible explanatory effects) by a small nonthermal electron population, if the temperature of this population is sufficiently high. It is to be noted that such very high temperature nonthermal electrons should be located in the plasma and should not drift far into the SOL (the last closed flux surface, determined from the floating potential profile, is at 73 mm in figure 2). If nonthermal electrons would be causing the difference in measured T_e-values between TP and LP, those T_e-measurements should be in agreement with each other inside the SOL, which is clearly not the case in figure 2. Another symptom of the presence of the nonthermal electrons would be the non-saturation of the ion current on the I–V characteristics of the swept TP. Again, none of the characteristics used in figure 2 showed this behaviour. In addition to this, for a scenario with highly energetic nonthermal electrons, the flow of nonthermal electron current to the BP is going to be the dominant mechanism altering the TP T_e-measurement, which means that the sensitivity of the TP measurement to the nonthermal electrons should strongly depend on the TP biasing voltage. However, as is clear from figure 2, for the deeper radial positions where TP $T_e \sim 10$ eV and $J_\parallel \sim 10\,000$ A m^{-2} and the conditions are thus comparable to those of the simulated cases (*a*), (*b*), (*c*) and (*d*) in figure 3, the TP measurement results for different biasing voltages are, within the error bars, equal to each other. This excludes the presence during those measurements of nonthermal electrons which are sufficiently hot to fully explain the difference between the TP and the LP values. This means that the strong difference between the LP and the TP values cannot be satisfactorily explained by nonthermal electrons only.

It can also be pointed out that, even if probably no very hot nonthermal electron populations were influencing the TP measurements in CASTOR presented in this paper, it is advisable to operate the TP at voltages as negative as possible. This should be done to exclude as much as feasible any potential effects of very high-temperature nonthermal electron populations on the TP measurements. For CASTOR measurements, the TP is therefore only operated in dc at $V_{bias} = -200$, if possible.

Decreasing $J_\parallel$ results in an increase in the TP sensitivity to a high temperature nonthermal electron component, as illustrated in figure 3(*e*). For sufficiently high $F_{e^-,supr}$-values, the TP can be even more sensitive than the LP. Again we notice the dominating effect of the nonthermal electron current to the BP ($I_{e^-,supr,BP}$). This increase in sensitivity is found to be caused by the precise difference in balance of two opposite effects at the two levels of $J_\parallel$ (2500 A m^{-2} and 10 000 A m^{-2}). An electron current to the BP results in a decrease in the measured I_{BP}, thus lowering the total measured current ($I_{TUN} + I_{BP}$) but increasing R_c. According to the calibration simulation results shown in figure 1, an underestimation of $J_\parallel$ will lead to a lower $T_{e,measured}$, while an overestimation of R_c will have the opposite effect. A detailed investigation of the calibration curves shows that for the specific plasma parameters in figure 3(*e*), the latter effect is indeed prevailing. This $J_\parallel$ dependence of the difference in sensitivity of the TP to

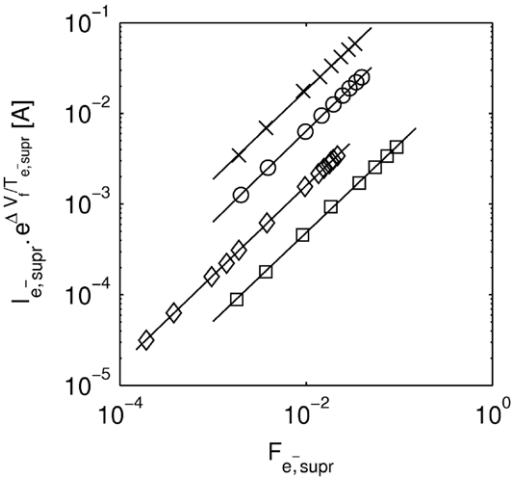

Figure 5. e^-_{supra} current to the BP, corrected for the difference in floating potential caused by the presence of the e^-_{supra}, as a function of the density fraction of e^-_{supra}. The depicted cases have $T_{e,therm} = 10\,eV$ in common and are further specified by $J_\parallel = 10\,000\,A\,m^{-2}$, $T_{e,supr} = 100\,eV$, $V_{TP,bias} = -100\,V$ (crosses), $J_\parallel = 10\,000\,A\,m^{-2}$, $T_{e,supr} = 100\,eV$, $V_{TP,bias} = -200\,V$ (circles), $J_\parallel = 2500\,A\,m^{-2}$, $T_{e,supr} = 100\,eV$, $V_{TP,bias} = -200\,V$ (diamonds) and $J_\parallel = 10\,000\,A\,m^{-2}$, $T_{e,supr} = 50\,eV$, $V_{TP,bias} = -200\,V$ (squares). Those cases correspond with the cases (*d*), (*a*), (*e*) and (*b*) (respectively) of figure 3.

nonthermal electrons is also not observed in the radial profile of figure 2, again indicating that the difference between TP and LP T_e-measurement results cannot be explained entirely by the possible presence of nonthermal electrons.

At a TP biasing voltage of $-200\,V$ and with $J_\parallel = 2500\,A\,m^{-2}$ and nonthermal electrons at 20 eV, as illustrated in figure 3(*f*), no electrons can reach the BP. Consequently their effect on the TP T_e-measurements is, just like for the analogous case at $J_\parallel = 10\,000\,A\,m^{-2}$, entirely due to the change in the ratio of the ion current to the tunnel and the BP (R_{ion}), which is a result of the modification of $\boldsymbol{E}$ by the fast electrons.

Although the potential presence of a population of nonthermal electrons cannot on its own fully explain the difference between the T_e-values obtained with LP and TP, it might still be a contributing factor in an explanation which combines multiple effects. Another explicative mechanism could be e.g. secondary electron emission at the BP of the TP. This justifies a more detailed analysis of the effect of a population of nonthermal electrons on the TP. Given that for small nonthermal electron populations changes in $I_{e^-,supr,BP}$ are the dominant mechanism altering the TP T_e-measurements, it is worth studying how this quantity depends on the probe and plasma parameters. This may allow us to model its behaviour such as to reduce as much as possible the number of numerical simulations required to determine the influence on the TP of nonthermal electrons under specific circumstances. More specifically, we could think of deriving the dependence of the TP T_e measurement on $F_{e^-,supr}$ for one of the cases in figure 3 using the simulation results of any other depicted case.

4. Scaling of the nonthermal electron current to the back plate

$I_{e^-,supr,BP}$ is studied in more detail in figure 5. $I_{e^-,supr,BP}$ is multiplied with a Boltzmann factor to correct for the differences in floating potential between the simulations with different levels

Table 1. Parameters obtained from the fit to $I_{e^-,\mathrm{supr,BP}}$ as a function of $F_{e^-,\mathrm{supr}}$ for different plasma conditions and tunnel probe voltages.

Case in figure 3	$V_{\mathrm{bias,TP}}$ (V)	$T_{e^-,\mathrm{supr}}$ (eV)	$J_\parallel$ (A m^{-2})	a	b
(a)	−200	100	10 000	0.871	1.002
(b)	−200	50	10 000	0.046	0.978
(d)	−100	100	10 000	2.319	0.983
(e)	−200	100	2 500	0.211	0.991

of nonthermal density fraction and plotted as a function of $F_{e^-,\mathrm{supr}}$ for cases (*a*), (*b*), (*d*) and (*e*) of figure 3. For each case a fit of the form $y = ax^b$ was made. The resulting fitted parameters are given in table 1.

From figure 5 and table 1 it is clear that $I_{e^-,\mathrm{supr,BP}}$ has a Boltzmann factor dependence on the voltage difference between the injection plane and the BP, as confirmed by the ratio of the BP electron currents at −200 V and −100 V (which is $\sim \exp(-100\,\mathrm{V}/k100\,\mathrm{eV})$, with k being the Boltzmann constant). It is also evident that $I_{e^-,\mathrm{supr,BP}}$, after corrections for different V_f, scales linearly with $F_{e^-,\mathrm{supr}}$ (as the fitted b-values in table 1 are ~ 1) and with $J_\parallel$ (the fitted a-parameter for case (*a*) in table 1 is around 4 times the a-value for case (*e*)). However, contrary to what one may perhaps expect, there is no Boltzmann factor dependence as far as the temperatures of the nonthermal electron populations are concerned (as illustrated by cases (*a*) and (*b*)).

Given that for a nonthermal electron population at 100 eV, $I_{e^-,\mathrm{supr,BP}}$ plays the dominant role as compared with the changes in R_ion, we can now attempt to reproduce the TP curves of cases (*d*) and (*e*) in figure 3 starting from the numerical simulation results from the case of figure 3(*a*) and the undisturbed ion current distributions of (*d*) and (*e*). The results of this exercise are plotted in graph (*d*) and (*e*) of figure 3 as crosses connected by dotted lines. We notice that the curves are reproduced fairly well, except for a small deviation that can be attributed to the changes in R_ion.

5. Summary and conclusions

During experiments in the CASTOR tokamak, the T_e-values measured with the tunnel probe were found to be several times lower than those obtained using a Langmuir probe interpretation of the tunnel probe I–V characteristic. As a non-Maxwellian velocity distribution of the electrons could be a possible explanation for this discrepancy between TP and LP, the influence of the presence of a nonthermal electron component on the TP has been studied using the XOOPIC code. It was found that this influence depends on the temperature of the nonthermal electron population, on the biasing voltage of the TP and on the parallel ion current density.

The presence of very hot nonthermal electrons can be detected by looking at the negative voltage part of the I–V characteristics of the swept probe: it should show no hard saturation of the ion current. The CASTOR TP data presented here were carefully checked for this sign but it was not observed. In addition to this, the comparison of the simulation-derived dependences with radial LP and TP T_e-profiles which were measured in CASTOR makes it clear that the difference between TP and LP T_e-measurement results cannot be explained exclusively by the possible presence of nonthermal electrons. Nevertheless, it might still be a contributing factor in an explanation which combines multiple effects. For instance, in [8] it was assumed that the Langmuir probe temperature was correct and that the tunnel probe measurement was too low because of ion induced secondary electron emission from the BP. In order to make the

two measurements agree, it was found that a secondary emission coefficient of 0.5 would be needed. Published data from the literature indicate emission coefficients in the range of 0.3–0.4 for dirty copper [17]. If one uses these coefficients to correct the BP current, the TP estimate of T_e increases but still remains lower than the LP estimate. The remaining discrepancy could be due to nonthermal electrons.

Nonthermal electrons exert their influence through a combination of two mechanisms: highly energetic electrons can reach the BP and alter the measured BP current directly while the presence of a certain density fraction of nonthermal electrons will also influence the ion current distribution over the tunnel and BP. The electron current to the BP scales, after corrections for different V_f, linearly with $F_{e^-,supr}$ and $J_\parallel$ and has a Boltzmann factor dependence on the voltage difference between the injection plane and the BP.

The principal result of this study is that Langmuir probes and tunnel probes behave differently in the presence of nonthermal electrons. Therefore, comparing the two types of measurements can potentially provide a tool to investigate the characteristics of the electron distribution in the edge plasma of magnetic fusion devices.

References

[1] Van Oost G 2003 *Plasma Phys. Control. Fusion* **45** 621–43
[2] Gunn J P 2001 *Phys. Plasmas* **8** 1040
[3] Gunn J P *et al* 2002 *Czech. J. Phys.* **52** 1107
[4] Gunn J P *et al* 2004 *Rev. Sci. Instrum.* **75** 4328
[5] Gunn J P 1997 *Phys. Plasmas* **4** 4435
[6] Chodura R 1982 *Phys. Fluids* **25** 1628
[7] Verboncoeur J P, Langdon A B and Gladd N T 1995 *Comput. Phys. Commun.* **87** 199
[8] Gunn J P, Panek R, Stöckel J, Van Oost G and Van Rompuy T 2005 *Czech. J. Phys.* **55** 255
[9] Stangeby P C 1995 *Plasma Phys. Control. Fusion* **37** 1031
[10] Shoucri M, Shkarofsky I, Stansfield B, Boucher C, Pacher G and Décoste R 1998 *Contrib. Plasma Phys.* **38** 225
[11] Batishchev O V *et al* 1997 *Phys. Plasmas* **4** 1672
[12] Dejarnac R 2007 private communication
[13] Birdsall C K and Langdon A B 1985 *Plasma Physics via Computer Simulation* (New-York: McGraw-Hill)
[14] Stangeby P C 1984 *J. Nucl. Mater.* **128–129** 969
[15] Riemann K-U 1995 *IEEE Trans. Plasma Sci.* **23** 709
[16] Godyak V A, Piejak R B and Alexandrovich B M 1993 *J. Appl. Phys.* **73** 3657
[17] Kyslyakov A I *et al* 1975 *Zh. Tekh. Fiz.* **7** 1545 (in Russian)